

Experimental Study on Two-Phase Pressure Drop through Horizontal Mini-Channel with Y-Branch

R. Nagai*, Y. Tabata, M. Sadatomi, A. Kawahara, A. Santoso

Department of Advanced Mechanical Systems, Graduate School of Science and Technology, Kumamoto University, Japan

Abstract The present study is concerned with the pressure loss due to 60 degree Y-branch in horizontal mini-channel with a rectangular cross-section of 2.5 mm height \times 4.6 mm width in the upstream channel and of 2.5 mm height \times 2.36 mm width in the downstream channels. The pressure loss, the gas phase velocity and the void fraction in the channels upstream and downstream from the branch were measured, and analysed. Since no correlations of the respective parameters has found, the new correlations has been proposed and their validity against the present experimental data has been clarified.

Keywords Rectangular mini-channel, Two-phase flow, Y-branch, Pressure drop

1. Background

Gas-liquid two-phase flow in mini-channels is a phenomenon seen in compact chemical reactors and heat exchangers with phase change, e.g., air conditioners and cooling devices. These devices contain flow channels of various cross-sections, e.g., circular and rectangular, as well as various types of singularities, e.g., branches, sudden expansions, sudden contractions, bend, and so on. In particular, there are many configurations of the branches, i.e., the impacting T-junction and the side branches with various angles. In order to design and develop the mini-size heat exchanger with the side branches, a full understanding of the characteristics of two-phase flow through the branch and the pressure gradient in the channels upward and downward from the branch in various flow regimes is essential.

Ito and Imai (1973) measured the single-phase pressure drop in equal-sided impacting T-junctions of circular cross-section of 35 mm I.D. with various curvature radii and geometrical shapes of joining edge. The experiments were conducted at two inlet Reynolds numbers of $Re = 1 \times 10^5$ and 2×10^5 . They reported a correlation for the pressure loss coefficient as a function of the split ratio and the curvature radius and the joining edge. Oka and Ito (2005) studied tees and wyes with the large area ratios of the inlet channel to the outlet channel. For the tees, the test section had an inlet channel of 54.03 mm I.D. and outlet ones of two different sizes of 54.03 mm and 15.97 mm. All

experiments were conducted with a fixed inlet Reynolds number of $Re = 1 \times 10^5$. A correlation was proposed for the pressure loss coefficient through the tee as a function of the split ratio and the inlet to outlet area ratio. Elazhary and Soliman (2012) studied the single- and two-phase pressure drops in a horizontal mini-channel with an impacting T-junction with a rectangular cross-section of 1.87 mm height \times 20 mm width. The correlations for the single-phase and two-phase pressure losses were proposed relating to the inlet flow rates of gas and liquid, the split ratio. All these studies are concerned with impacting T-junctions and there are a few on the studies on the two-phase flows through Y-branch, and nothing on mini-channels with the Y-branch.

The first objective of the present study is to obtain experimental data on the pressure distribution along the test channel with 60 degree Y-branch with a rectangular cross-section, the gas phase velocity and the void fraction in the channels upstream and downstream from the branch. The channel is mini sized one placed on a horizontal plane and has dimensions of 2.5 mm height \times 4.6 mm width in the upstream channel and of 2.5 mm height \times 2.36 mm width in the downstream channel. The second one is to analyse the data with models and correlations relating to the data to determine their accuracy in prediction. The third one is to propose the respective new correlations. A result of such experiment, analysis and proposal is described in the present paper.

2. Experimental Method

2.1. Experimental Apparatus

Figure 1 shows a top view of the present mini test channel with Y-branch placed on a horizontal plane. The

* Corresponding author:

145d8545@st.kumamoto-u.ac.jp (R. Nagai)

Published online at <http://journal.sapub.org/jmea>

Copyright © 2016 Scientific & Academic Publishing. All Rights Reserved

test channel has a rectangular cross-section, and is made of transparent acrylic resin for visual observation.

Table 1 shows the cross-sectional dimensions of the channel cross-section: the width (W), height (H) and the hydraulic diameter (D_H). They are 4.60 mm, 2.50 mm and 3.24 mm for the upstream Ch.1, while 2.36 mm, 2.50 mm and 2.44 mm for the downstream Ch. 2 and Ch. 3, thus the ratio of contraction σ_A is approximately 0.52. Among 20 connecting taps, the tap #1 is the liquid phase inlet port while the taps #2 and #3 are the gas phase inlet ports.

Therefore, the gas-liquid two-phase flow starts from section 1. The taps #4 and #5 are the outlet ports of the flow. P_1 to P_{15} are the pressure taps, and the pressure at P_4 was measured with a gauge type pressure transducer (FP101-L31-L20, Yokogawa). The pressure at other pressure tap was determined from the pressure difference measured with a differential pressure transducer (DP15-32 and DP15-26 depending on the pressure range) between the tap and P_4 tap. The accuracy of the pressure measurement was confirmed within 3.5 Pa from a calibration test.

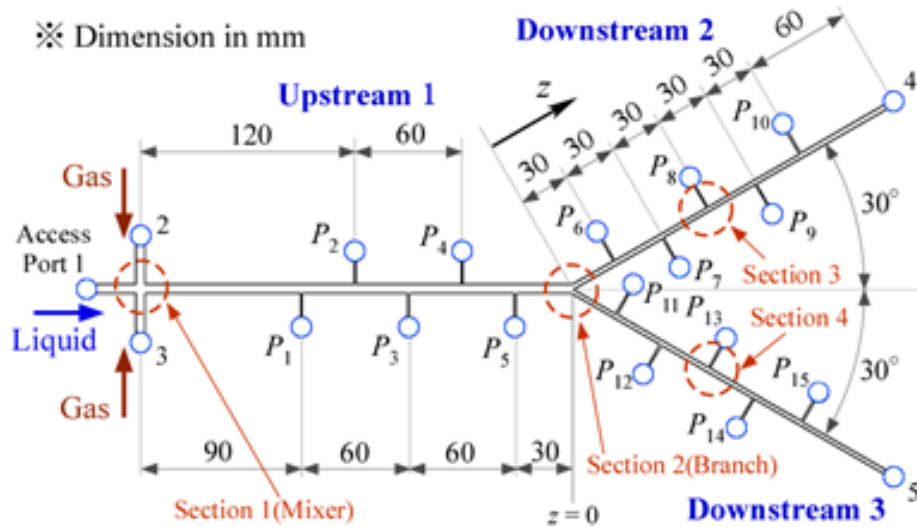


Figure 1. Top view of mini test channel with Y-branch

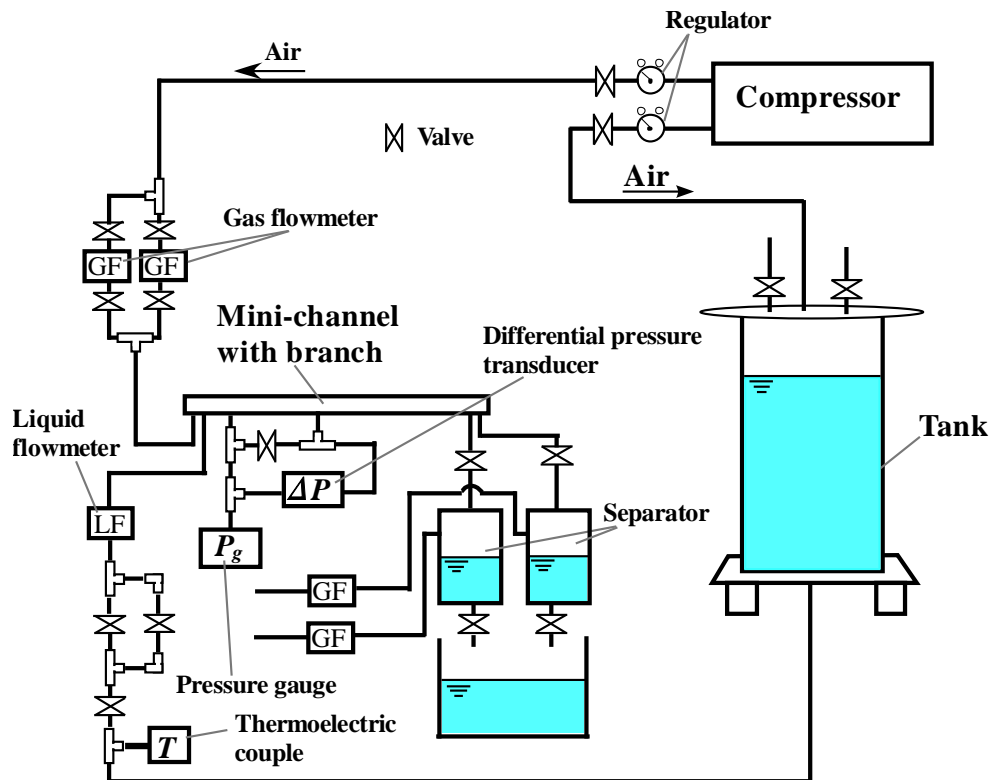


Figure 2. Experimental apparatus

Table 1. Channel width, height and hydraulic diameter, respectively for Ch. 1 to 3

| | W [mm] | H [mm] | D_H [mm] |
|----------------------|----------|----------|------------|
| Upstream Ch. 1 | 4.60 | 2.50 | 3.24 |
| Downstream Ch. 2 & 3 | 2.36 | 2.50 | 2.44 |

Figure 2 shows the present apparatus. Water as the test liquid was introduced from a tank to the test channel by a pneumatic-type pump via a flow control valve and a liquid flowmeter. The pump consisted of a pressure vessel containing water and pressurized air from a compressor for pushing the water surface in the vessel. This pump gave a steady pulsation-free liquid flow. Air as the test gas was introduced from a compressor to the test channel via a pressure regulator, a flow control valve, and a gas flow meter.

The liquid and the gas flow rates introduced were read from calibrated mass flow meters (FD-S and FD-A1, both KEYENCE Co., Ltd.). In order to obtain accurate time averaged values of air and water flow rates and pressures, the output signals from the respective sensors were fed to a personal computer via A/D converter at nominally 1 kHz over 10 sec. The liquid flown from the outlet of Ch. 2 and 3 were separated from air in the respective separators, and their flow rates were measured by weighting the liquid discharged over a sufficient period of time using a small container and an electric balance (200 ± 0.001 g, SHIMADZU Co). The liquid split ratio from Ch. 1 to Ch. 3, $R_L = Q_{L3}/Q_{L1}$, was controlled with a flow control valve between the outlet of Ch. 2 and the separator for Ch. 2, by taking care of the water levels in the separators of Ch. 2 and 3 to remain the same height. The airs separated in the respective separators were lead to the respective dry-type gas volumetric flow meters. In order to confirm the accuracy of the respective outflows, the authors checked the total mass flow rate of Ch. 2 and 3 to agree with the mass flow rate of Ch. 1, respectively for water and air. If the agreement was worse than 10 % to the flow rate of Ch. 1, the data was discarded.

The flows in three observation area of section #3 (Ch. 1), section #4 (Ch. 2) and section #5 (Ch. 3) in Fig. 1 were observed with a high-speed video camera (VH-Z00R, KEYENCE Co., Ltd.) in order to determine the respective flow patterns.

Besides the above measurements, the gas phase velocity, u_G , in two-phase flow was measured with the high-speed video camera, and the void fraction, α , was determined by substituting the measured u_G and the superficial gas velocity, $j_G (= Q_G / (W \cdot H))$, into $\alpha = j_G / u_G$.

2.2. Experimental Conditions

The ranges of the liquid and the gas superficial velocities, $j_{L,1}$, $j_{G,1}$ at $z = -30$ mm, a point 30 mm upstream from the Y-branch and the liquid split ratio, R_L , in the present experiments are listed in Table 2. The superficial velocity is the volume flow rate divided by cross-sectional area of flow channel. Since the static pressure dropped gradually from the channel inlet to outlet, the superficial velocity of gas, j_G , increased along the channel axis. Thus, j_G , at $z = -30$ mm in Ch. 1, $z = 30$ mm in Ch. 2 and Ch. 3 were used in the discussion of gas phase velocity and void fraction data. Flow regimes covered are all slug flows in Ch. 1 but include a little bubble flow in Ch. 2 and 3.

3. Results and discussion

3.1. Gas Phase Velocity and Void Fraction

The gas phase velocity, u_G , data for all channels were plotted against the total superficial velocity, $j (= j_G + j_L)$ as shown in Fig. 3. The solid and broken lines represent the calculations by the following homogeneous flow model, Eq. (1), and drift flux model by Zuber and Findlay (1965), Eq. (2), with Mishima and Hibiki's C_0 correlation (1996), Eq. (3):

$$u_G = j (= j_G + j_L). \quad (1)$$

$$u_G = C_0 j + V_{Gj}. \quad (2)$$

$$C_0 = 1.2 + 0.510 \exp(-0.091 D). \quad (3)$$

Here, the drift velocity, V_{Gj} , was taken as zero since the flow is horizontal. Eq. (3) was based on air-water two-phase flow data in vertical circular pipes of 1 to 5 mm I.D., where D is the inner diameter of the pipe in mm. In the present study, D was replaced by the hydraulic diameter, D_H , because of rectangular channel.

The u_G data distribute a little higher than the line of homogeneous flow model ($u_G = j$), but do not agree with $u_G = 1.63 j$. Thus, the distribution parameter, C_0 , was modified as follows:

$$C_0 = 0.63(1.2 + 0.510 \exp(-0.091 D_H)). \quad (4)$$

Fig. 4 shows that the calculated u_G by Eqs. (2) and (4) agree with the present data within 12% in average for all channels.

Table 2. Flow and temperature conditions of the present experiments

| j_{G1} [m/s] | j_{L1} [m/s] | Re_{G1} [-] | Re_{L1} [-] | T_G [°C] | T_L [°C] | $R_L = Q_{L3}/Q_{L1}$ |
|----------------|----------------|---------------|---------------|------------|------------|-----------------------|
| 0.5-1.0 | 0.5-1.25 | 110-250 | 1800-4800 | 26.1-31.8 | 25.8-31.2 | 0.2-0.5 |

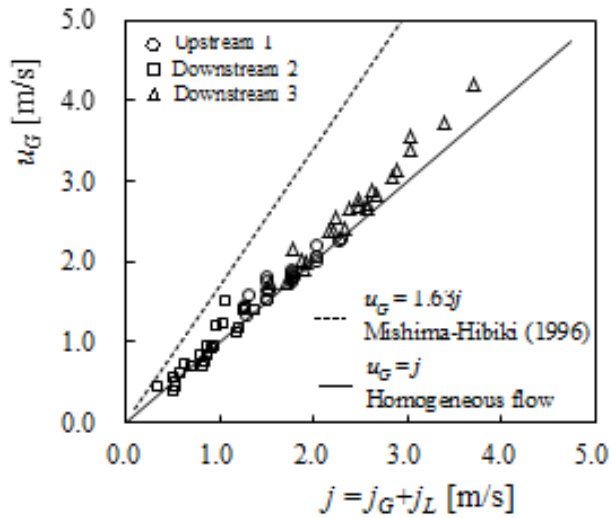


Figure 3. Gas phase velocity data for Ch.1, Ch.2 and 3 against total superficial velocity

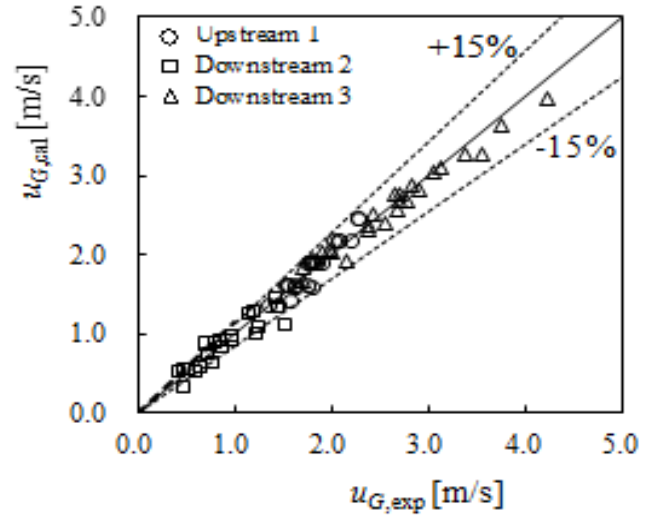
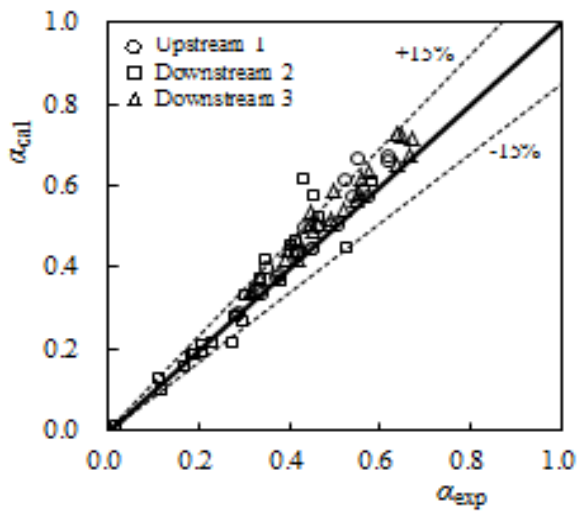
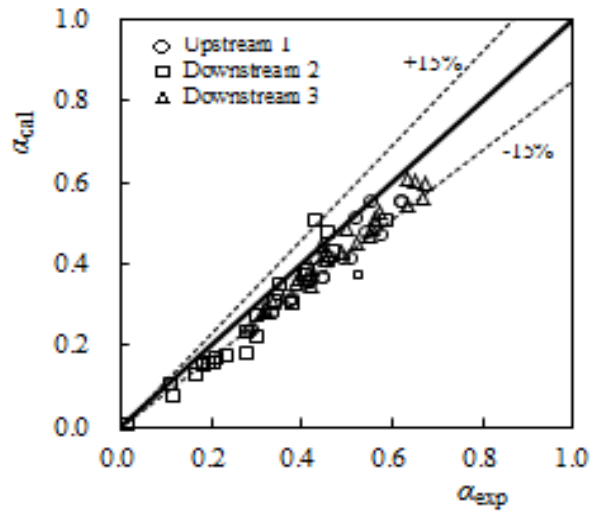


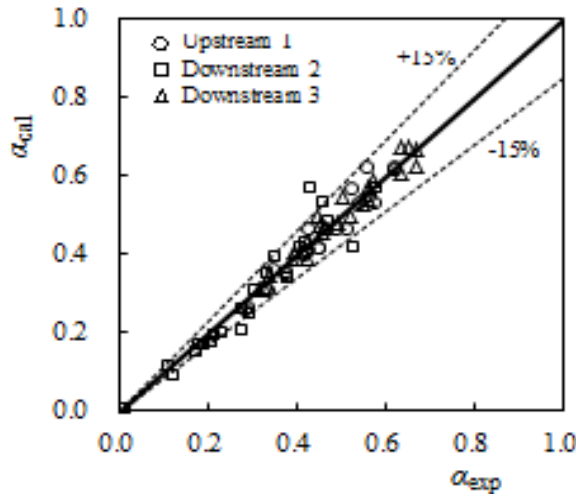
Figure 4. Comparison of gas phase velocity between experiment and calculation by drift flux model with Eq. (4) for the distribution parameter



(a)



(b)



(c)

Figure 5. Comparison of void fraction between experiment and calculations by three correlations (a) Homogeneous low model, (b) Armand's correlation, (c) The Present correlation

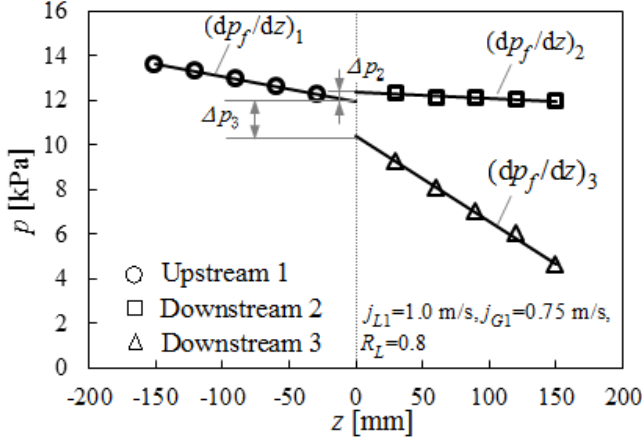


Figure 6. Pressure distribution along the channel axis

The void fraction, α , data was obtained by substituting u_G data into $\alpha = j_G/u_G$. These data are compared with the following three correlations: (a) homogeneous flow model ($\alpha = \beta$), (b) Armand's correlation (1946), $\alpha = 0.833\beta$, and (c) the present correlation using Eqs. (2) and (4). Where $\beta (= j_G/j)$ is the gas volume flow fraction. Figs. 5 (a) – (c) show the assessment results of the three void fraction correlations. In a low void fraction range, the data agree well with the calculation by the homogeneous flow model. While in a high void fraction range, the data agree well with the calculation by the present correlation.

The prediction errors by each correlation are 7.5%, -10.4%, and 0.1% for the average relative error, ε_M , and 12.7%, 13.5% and 9.5% for the root mean square error, ε_{RMS} .

$$\varepsilon_M = \frac{1}{N} \sum_{i=1}^N \left(\frac{\alpha_{cal,i} - \alpha_{exp}}{\alpha_{exp}} \right), \quad \varepsilon_{RMS} = \left[\frac{1}{N-1} \sum_{i=1}^N \left(\frac{\alpha_{cal,i} - \alpha_{exp}}{\alpha_{exp}} \right)^2 \right]^{0.5}. \quad (5)$$

Here, N is the number of the data points. The minimum errors for the whole data were obtained by the present correlation.

3.2. Axial Pressure Distribution and Branch Pressure Drop

Figure 6 shows typical results on the axial pressure distributions measured for a slug flow at $j_{G1} = 0.75$ m/s and $j_{L1} = 1.0$ m/s, and at the split ratio of liquid of $R_L = 0.8$. The gradient of two-phase frictional pressure drop in Ch. 1, Ch. 2 and 3, $(dp_f/dz)_1$, $(dp_f/dz)_2$ and $(dp_f/dz)_3$, is obtained by fitting the pressure distribution data in each channel with the least-square method. The pressure changes across the Y-branch, Δp_2 and Δp_3 , the pressure changes between Ch. 1 and 2 and Ch.1 and 3, are determined by the extrapolations of the respective pressure distributions. In the present paper, Δp_3 is used as the representative because the Δp_2 is relatively small and tend to have a poor accuracy.

The pressure change, Δp , is the sum of the reversible and the irreversible changes, Δp_R and Δp_{Ir}

$$\Delta p = \Delta p_R + \Delta p_{Ir} \quad (6)$$

$$\Delta p_R = \frac{1}{2} \left\{ \left[\rho_G \alpha_3 u_{G3}^2 + \rho_L (1 - \alpha_3) u_{L3}^2 \right] - \left[\rho_G \alpha_1 u_{G1}^2 + \rho_L (1 - \alpha_1) u_{L1}^2 \right] \right\}. \quad (7)$$

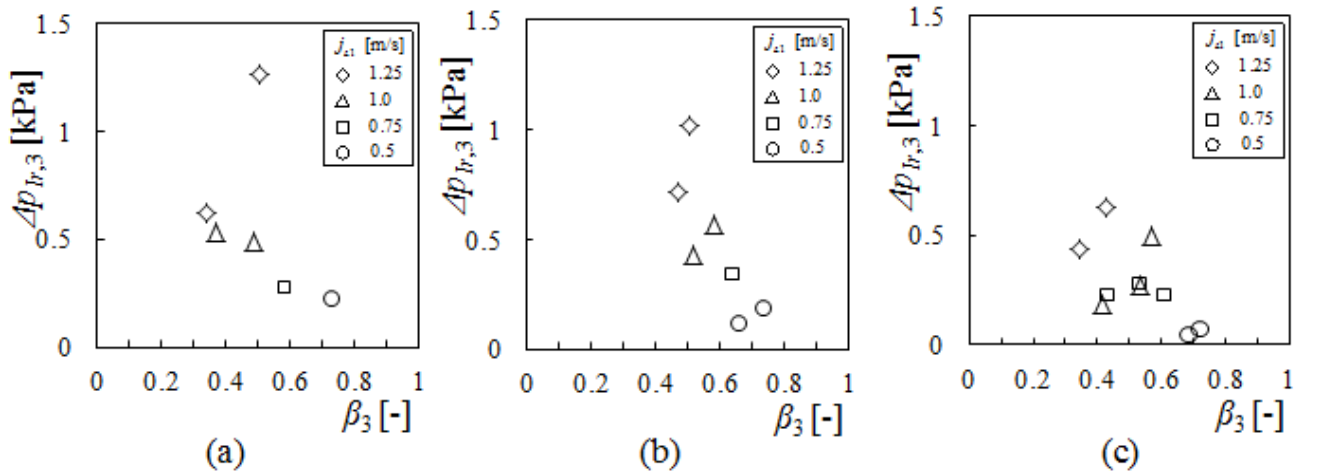


Figure 7. Irreversible pressure change at branch versus volumetric quality (a) $R_L = 0.8$, (b) $R_L = 0.7$, (c) $R_L = 0.6$

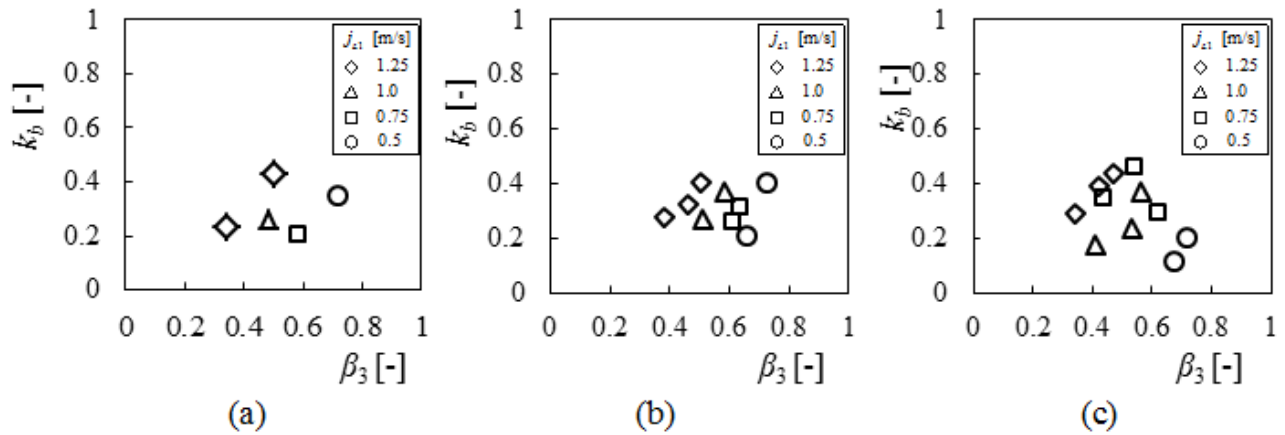


Figure 8. Pressure loss-coefficient against gas volumetric flow ratio (a) $R_L = 0.8$, (b) $R_L = 0.7$, (c) $R_L = 0.6$

Here, ρ_L and ρ_G are the liquid and air densities. In the present study, the terms relating air dynamic pressure in Eq. (7) are neglected because air density, ρ_G , is much smaller than the liquid density, ρ_L . The experimental data on the irreversible change, Δp_{Ir} , was determined from Δp data by subtracting calculated Δp_R .

Figures 7 (a) - (c) show the Δp_{Ir3} data for the branch from Ch.1 to Ch. 3 at three liquid split ratio of $R_L = 0.8, 0.7$ and 0.6 . The abscissa is the volumetric quality at Ch. 3. The symbols in each figure are labelled depending on liquid superficial velocity in Ch. 1, j_{L1} . Δp_{Ir3} increases with increasing of j_{L1} at a fixed R_L and β_3 . In addition, at a fixed j_{L1} , Δp_{Ir3} is roughly constant and independent of β_3 .

In the present study, the branch pressure loss-coefficient, k_b , is defined as:

$$k_b = \frac{\Delta p_3 - \Delta p_R}{(1 - \alpha_3) \frac{\rho_L u_{L3}^2}{2}} \quad (8)$$

The branch loss-coefficient data is plotted against the volumetric quality in Ch. 3 in Figs. 8 (a) - (c) for each R_L . Although Δp_{Ir3} data depend on j_{L1} as the mentioned above, but k_b data do not dependent so much on j_{L1} and are roughly constant of $k_b = 0.30$.

3.3. Prediction of Irreversible Pressure Loss at Branch

If the inlet and the outlet gas and liquid superficial velocities and liquid physical properties are given, the irreversible pressure loss due to the branch, Δp_{Ir} , can be predicted from Eq. (9), being the same as Eq. (8), with $k_b = 0.3$ together with Eqs. (2) and (4) for u_G calculation.

$$(\Delta p_{Ir})_{cal} = k_b (1 - \alpha_3) \frac{\rho_L u_L^2}{2} \quad (9)$$

In order to validate the present prediction method on the two-phase irreversible pressure loss due to the branch, the calculation value, $(\Delta p_{Ir})_{cal}$ was compared with the present data, $(\Delta p_{Ir})_{exp}$. The average error and the root mean square error of $((\Delta p_{Ir})_{cal} - (\Delta p_{Ir})_{exp}) / (\Delta p_{Ir})_{exp}$ are 17.2% and 45.4%. Figure 9 shows the comparison between the experiment and

the calculation. In the case of $j_{L1} = 0.5$ m/s, the average of relative error is 45.7% and root mean square of that is 88.9%, while in the case of other j_{L1} , the average of relative error is 8.6% and root mean square of that is 28.5%. Therefore, it can be concluded that the present method can predict the irreversible pressure loss due to the branch within r.m.s. error of 28.5% if $j_{L1} \geq 0.75$ m/s.

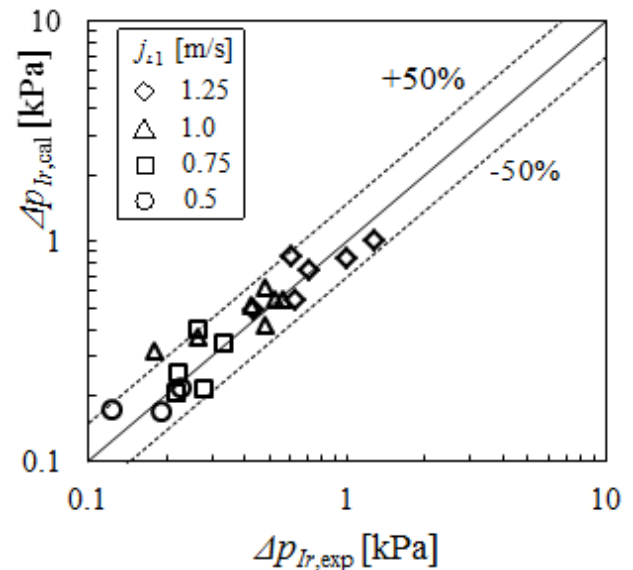


Figure 9. Comparison of irreversible pressure loss between the present calculation and the present experimental data

4. Conclusions

Air-water two-phase flow experiment was conducted at room temperature and atmospheric pressure using a horizontal rectangular mini-channel with a Y-branch. The width and height were from 4.6 mm by 2.5 mm to 2.36 mm by 2.5 mm. From the analyses of the experimental data, the followings can be clarified:

1. The gas phase velocity data did not fit well the calculations by the homogeneous flow model and the drift flux model with Mishima and Hibiki's C_0 correlation. However, by modifying C_0 correlation, the

calculation by the drift flux model agreed well with the present experiment data.

2. The void fraction prediction based on the above gas phase velocity calculation method agreed well with the experimental data within r.m.s error of 9.5 %.
3. The irreversible pressure loss-coefficient due to branch, k_b , was roughly constant of 0.30, independent of j_{L1} , β_3 and R_L .
4. The present calculation on the irreversible pressure loss due to the branch agreed with the present experimental data within r.m.s. error of 28.5% if $j_{L1} \geq 0.75$ m/s.

ACKNOWLEDGEMENTS

The present study was partially supported by KAKENHI (26420118).

REFERENCES

- [1] Ito, H., Imai, K. (1973). Energy losses at 90 ° pipe junctions. *ASCE J. Hydraulics Div.* 99, 1353 – 1368.
- [2] Oka, K., Ito, H. (2005). Energy losses at tees with large area ratios. *J. Fluids Eng.* 127, 110 – 116.
- [3] Elazhary, A. M., Soliman, H.M. (2012). Single- and two-phase pressure losses in a horizontal mini-size impacting tee junction with a rectangular cross-section. *Experimental Thermal and Fluid Science* 41, 67-76.
- [4] Zuber, N., Staub, & Findlay, J. A. (1965). Average Volumetric Concentration in Two Phase Flow Systems. *Trans, ASME, J. Heat Transfer*, 87, 453 -468.
- [5] Mishima, K., & Hibiki, T. (1996). Some Characteristics of Air-water Two-phase Flow in Small Diameter Vertical Tubes. *Int. J. Multiphase Flow*, 22 – 4, 703 – 712.
- [6] Armand, A. A. (1946). Resistance to Two-phase Flow in Horizontal Tube (in Russian). *Izv.VTI*, 15, 16 - 23.